Hindawi
Advances in Polymer Technology
Volume 2019, Article ID 5973403, 17 pages
https://doi.org/10.1155/2019/5973403

*Research Article*

# Study on External Gas-Assisted Mold Temperature Control for Improving the Melt Flow Length of Thin Rib Products in the Injection Molding Process

**Phan The Nhan,[1] Thanh Trung Do,[1] Tran Anh Son,[2] and Pham Son Minh[1]**

[1]*HCMC University of Technology and Education, Hochiminh City, Vietnam*
[2]*Ho Chi Minh City University of Technology, Vietnam*

Correspondence should be addressed to Pham Son Minh; minhps@hcmute.edu.vn

Received 20 December 2018; Revised 1 February 2019; Accepted 28 March 2019; Published 17 April 2019

Guest Editor: Jianzhang Li



In the injection molding process, mold temperature control is one of the most efficient methods for improving product quality. In this research, an external gas-assisted mold temperature control (Ex-GMTC) with gas temperature variation from 200°C to 400°C was applied to thin wall injection molding at melt thicknesses from 0.2 to 0.6 mm. The melt flow length was evaluated through the application of this system to the mold of a thin rib product. The results show that the heating process achieves high efficiency in the initial 20 s, with a maximum heating rate of 6.4°C/s. In this case, the mold surface reached 158.4°C. By applying Ex-GMTC to a 0.2 mm flow thickness, the flow length increased from 37.85 to 41.32 mm with polypropylene (PP) material and from 14.54 to 15.8 mm with acrylonitrile butadiene styrene (ABS) material. With the thin rib mold and use of Ex-GMTC, the mold temperature varied from 112.0°C to 140.8°C and the thin rib height reached 7.0 mm.

## 1. Introduction

Injection molding is a popular method for manufacturing plastic products. However, with consumer demands for higher product quality, as well as increasingly complex product geometries, it is clear that the injection molding process requires improvement. In this regard, mold temperature control is an effective method for solving issues encountered during the melt filling step [1–3]. In general, with a high mold surface temperature, component quality is improved; however, the cooling time and cycle time will both increase. By contrast, decreasing the mold surface temperature will reduce the cooling time but limit the surface quality of the component [4, 5]. Therefore, a critical requirement for current studies is to increase the mold surface temperature while maintaining a sufficiently short cycle time.

For the molding of micro products or products with thin walls, mold temperature should be set as high as the equipment allows. In the common molding process using a mold temperature controller, the mold temperature can be raised to about 90°C by hot water flowing inside the cooling channel [6]. However, in the field of electronic production using materials such as polycarbonate (PC) or polymethyl methacrylate (PMMA), the mold temperature must be higher than 100°C. In such cases, many different methods have been investigated for the purpose of raising mold temperature.

One common solution for cases where mold temperature must be higher than 100°C is the application of steam heating to the mold plate [7]. Although such a method is efficient in terms of the molding process and improving component quality, it may damage the channel and connector when operating at high pressure; energy use is also an issue. Use of an electronic heater inserted into the mold plate has also been suggested. The heater heats the mold cavity to the target temperature before the mold plate is cooled by the cooling channel. This method can heat the mold to higher than 100°C, but the heating time is an issue [8]. To improve the heating rate during mold temperature control, a thin heater has been adopted to control the temperature of cavity surfaces during the injection molding process. This method can support fast cooling even if it is kept active for very long periods. In experiments where the heater was set at 150°C

for a long heating period, the results showed a significant effect on sample frozen-in orientation, as identified by optical microscopy and confirmed by X-ray analysis. This method could be applied to micro injection molding with a suitable sheet heater [9]. However, in general, the electrical method often requires additional design and tool costs; this method also requires an auxiliary heating source.

To reduce energy wastage, surface heating methods have been studied. Chang et al. studied mold heating by infrared systems using simulations and experiments [10]. Their results showed that energy wastage was reduced. For a high heating rate, induction heating was investigated by Chen et al. [11], with the results illustrating that a large heating rate was achieved when using a suitable coil design. In addition, certain types of induction heating have been suggested such as proximity heating [12, 13] and ring coil heating [14]. However, with induction heating methods, there remain application difficulties, such as identifying the required coil design for reaching a good temperature distribution and the potential for overheating, which will damage the mold material. For directly heating the mold surface, gas-assisted mold temperature control (GMTC) has been suggested. With this approach, hot gas flows into the mold cavity. Through heat convection, the mold surface receives energy, increasing its temperature. In this method, the heating system includes gates inserted into the mold plate for hot gas entrance and exit [15, 16]. Initial results showed that the cavity surface could be heated to over 200°C. In addition, because hot gas flows into the cavity, this method can heat a complex cavity. However, the mold structure becomes more complex because of the combining of heating systems. Another disadvantage of GMTC is the temperature distribution; this is an issue that needs to be resolved.

Therefore, based on the disadvantages reported for GMTC, we applied external GMTC (Ex-GMTC) in which the gas temperature was varied from 200°C to 400°C. This was applied to thin wall injection molding at melt thicknesses of 0.2 to 0.6 mm. To improve the temperature distribution, the heating step was achieved using four gas gates on a melt flow length mold. In this case, the four gas gates were arranged along the cavity surface. After the molding process was complete, the length of the molding product was measured to observe the influence of Ex-GMTC on melt flow length. In addition, Ex-GMTC was applied to the injection mold of a thin rib product. In this application, the improvement of rib height was observed by heating the mold surface until the surface temperature was higher than the glass temperature of the material. In all cases, simulations were used to predict the heating rate and temperature distribution. Experimentally, mold temperatures were determined by infrared camera. The experiment and simulation results are compared and discussed.

## 2. Simulation and Experimental Methods

In general, the application of gas-assisted mold surface heating in injection molding is achieved using the six steps shown in Figure 1 [17]. According to this process, the mold cavity is heated to the target temperature before the hot melt is filled into the mold cavity. The greatest difference compared with the common injection molding process is the heating in Step 2. As with our former research on mold temperature control, hot gas was used as a heating source to increase the cavity surface temperature of the injection mold. Compared with other studies on gas heating for injection mold temperature control [15–17], Ex-GMTC is a new technique in the field of mold temperature control and can heat the cavity surface rapidly during the injection molding process without a significant change in the mold structure. During the heating operation, two mold plates are first moved to the open position by opening the mold. Second, a hot gas drier is moved to the heating position by a robot arm; then, the hot gas is sprued to directly contact the cavity surface. This hot gas heats the cavity surface to the target temperature. Third, after the cavity surface is heated to the target temperature, the gas drier is moved outside the molding area and the mold completely closes in preparation for the melt filling process.

In this research, the Ex-GMTC system consisted of a mold temperature controller, a hot gas generator system (including an air compressor, air drier with a power of 12 kW, and digital volumetric flow controller), and a robot arm for moving the hot gas generator system to the heating position. The assembly of the Ex-GMTC system and the injection molding machine is shown in Figure 2. For generating the hot air, the air drier was used with dimensions of 240 mm x 100 mm x 60 mm as shown in Figure 3. A gas channel, 5 mm in width and 10 mm in depth, was cut inside the gas drier. The environment air will press into the air drier with the pressure of 7 Bar; then, the air will flow along the gas channel and absorb the thermal energy from the wall of air channel. The hot air will flow out at the four gates with the hole diameter of 10 mm. The function of the high power hot gas generator system is to support a heat source, which provides a flow of hot air up to 400°C with an inlet gas pressure up to 7 Bar.

In this study, to observe the improvement of the melt flow length when using the Ex-GMTC, an injection mold was designed and manufactured with the structure of a cavity plate, as shown in Figure 4. In this case, the mold was designed with two cavities. One had the common structure and the other was designed with an insert, as shown in Figure 5. As with our previous research [15–17], this type of design helped to increase the heating efficiency and better control the heating area. The mold and the Ex-GMTC were assembled with a SW-120B molding machine from Shine Well Machinery Co., Ltd, as shown in Figure 6.

To study the temperature distribution of the heating area, a simulation model was built to represent the experiments. Because a cavity insert (Figure 5) was used, an insulation component covered the heating area; therefore, the simulation model includes only two volumes: the heating area volume and the hot gas volume, as shown in Figure 7. In contrast with former papers on gas-assisted temperature control for injection molding processes [15–17], the hot gas was sprued to the heating area via four gates to increase the temperature uniformity of the cavity surface. The simulation model and meshing model are shown in Figure 7, and the boundary conditions are shown in Table 1. To improve the

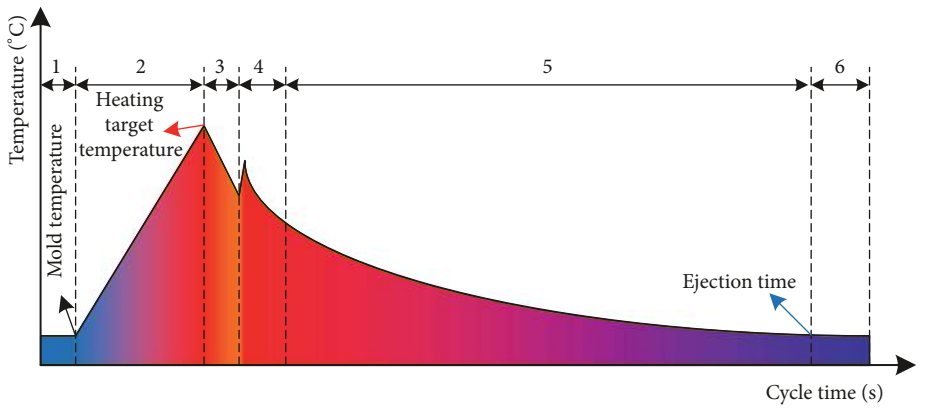


1. Mold closes to heating position
2. Hot gas heats the mold surface
3. Mold closes to molding position
4. Filling and packing process
5. Cooling process
6. Mold opens for part ejection

Figure 1: General process of gas-assisted mold surface heating in injection molding [17].

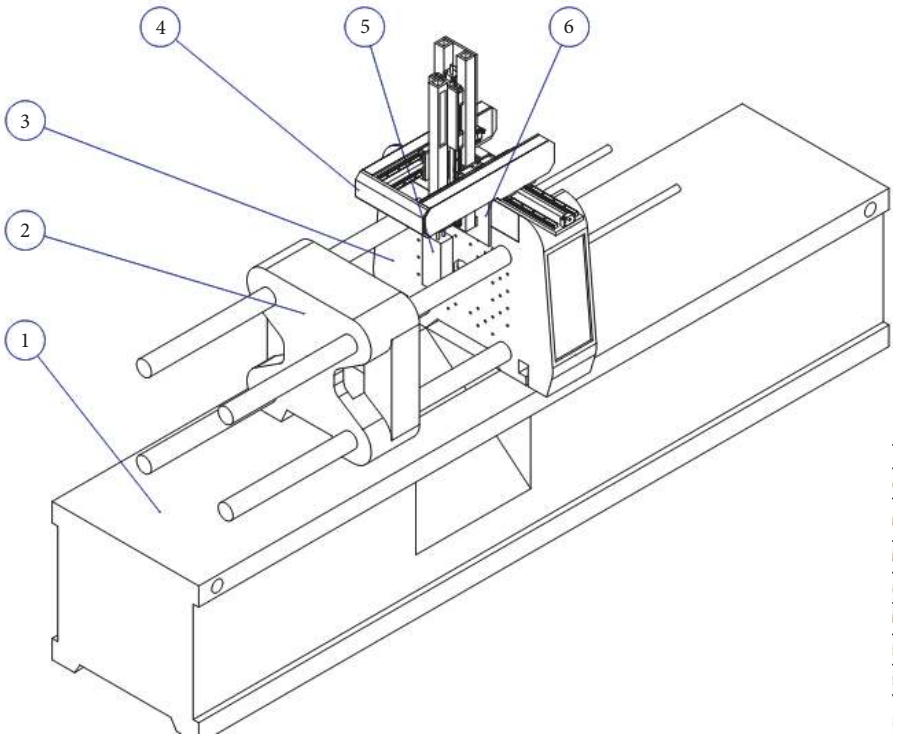


(1) Injection molding machine
(2) Core side
(3) Cavity side
(4) Robot arm
(5) Hot-gas generator
(6) The position for hang on the robot arm

Figure 2: External gas-assisted mold temperature control heating devices.

Table 1: Simulation parameters for studying melt flow length.

| Simulation parameters | | | | | | |
|---|---|---|---|---|---|---|
| Air inlet temperature of air drier | 30°C, 7 bar | | | | | |
| Air outlet temperature of air drier (°C) | 30 | 200 | 250 | 300 | 350 | 400 |
| Air density (kg/m$^3$) [18] | 1.165 | 0.746 | 0.680 | 0.616 | 0.570 | 0.524 |
| Heat capacity of air (J/kg∗K) [18] | 1004 | 1026 | 1035 | 1046 | 1057 | 1068 |
| Thermal-expansion coefficient of air (x10$^{-3}$K$^{-1}$) [18] | 3.32 | 2.1 | 1.93 | 1.76 | 1.64 | 1.52 |
| Air pressure | 1 atm | | | | | |
| Initial temperature of mold insert | 30°C | | | | | |
| Aluminum density - ASTM B209-14 | 2702 kg/m$^3$ | | | | | |
| Heat capacity of aluminum - ASTM B209-14 | 903 J/kg∗K | | | | | |
| Thermal conductivity of aluminum - ASTM B209-14 | 237 W/m∗K | | | | | |
| P20 steel density - ASTM A681 | 7870 kg/m$^3$ | | | | | |
| Heat capacity of P20 steel - ASTM A681 | 460 J/kg∗K | | | | | |
| Thermal conductivity of P20 steel - ASTM A681 | 29 W/m∗K | | | | | |
| Simulation type | Transient | | | | | |
| Heating time | 0 s ⟶ 30 s | | | | | |
| Air outlet to environment | (i) Environment pressure: 1 atm<br>(ii) Air temperature: 30°C | | | | | |
| Initial air volume | (i) Air velocity: 0 m/s<br>(ii) Air pressure: 1 atm<br>(iii) Air temperature: 30°C | | | | | |

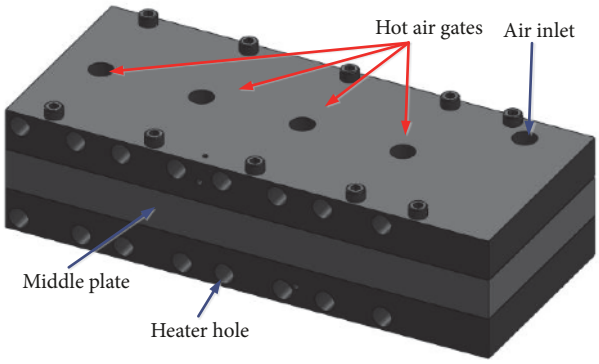


Figure 3: Air drier component parts.

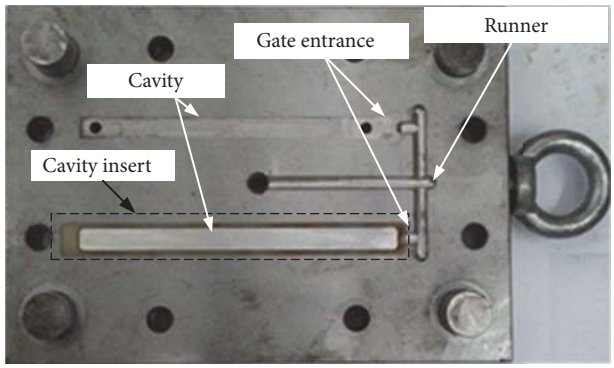


Figure 4: Cavity plate of melt flow length mold.

simulation accuracy, the cavity insert was meshed with a hex dominant element with seven layers in the thickness direction. In addition, with the air volume, a tetrahedron element used with a smaller element size was set up at the hot gas inlet location. The heating process was simulated by ANSYS software with the same experimental parameters.

After studying the influence of Ex-GMTC on the melt flow length of the injection molding process, this heating method was applied to a real product with a thin rib, as shown in Figure 8. The thin rib had a thickness varying from 0.5 to 0.3 mm and a height of 7.0 mm. This rib size is often used in plastic products for the electrical field. In many cases, a thin rib is used to increase the rigidness of the product; however, in the molding process, fully filling this type of rib is a challenge of rapid cooling of the melt as it enters the cavity. To improve the process of filling melt into a thin rib, Ex-GMTC was applied using one gate of hot gas. The heating area and the cavity structure are shown in Figure 9. The hot gas was sprued directly on the center of the heating area. Then, the temperature distribution and temperature values at three points, as shown in Figure 9, were collected. For observing the temperature distribution along the thickness of mold, a 3D thermal fluid analysis was performed by ANSYS software. Figure 10 shows the simulation model of the thin rib mold. In simulation, the heat transfer mode around all external surfaces of mold plate was set at free convection to the air, with ambient temperature at 30°C and a heat transfer coefficient of 10 W/m2 K. The same with experiment, the area at the cavity center was designed with a steel insert to improve the heating efficiency. This cavity insert had dimensions of 40 × 25 × 1.0 mm$^3$. A 400°C gas inlet was used for simulation.

## 3. Results and Discussion

*3.1. Effect of External Gas-Assisted Mold Temperature Control on the Heating Process of a Melt Flow Length Mold.* In our former research [15–17], when hot gas was used to raise cavity temperature, heating efficiency was relatively good. However, in addition to the disadvantage of the complex mold structure, the temperature distribution within the cavity is an issue in need of further research. Therefore, in

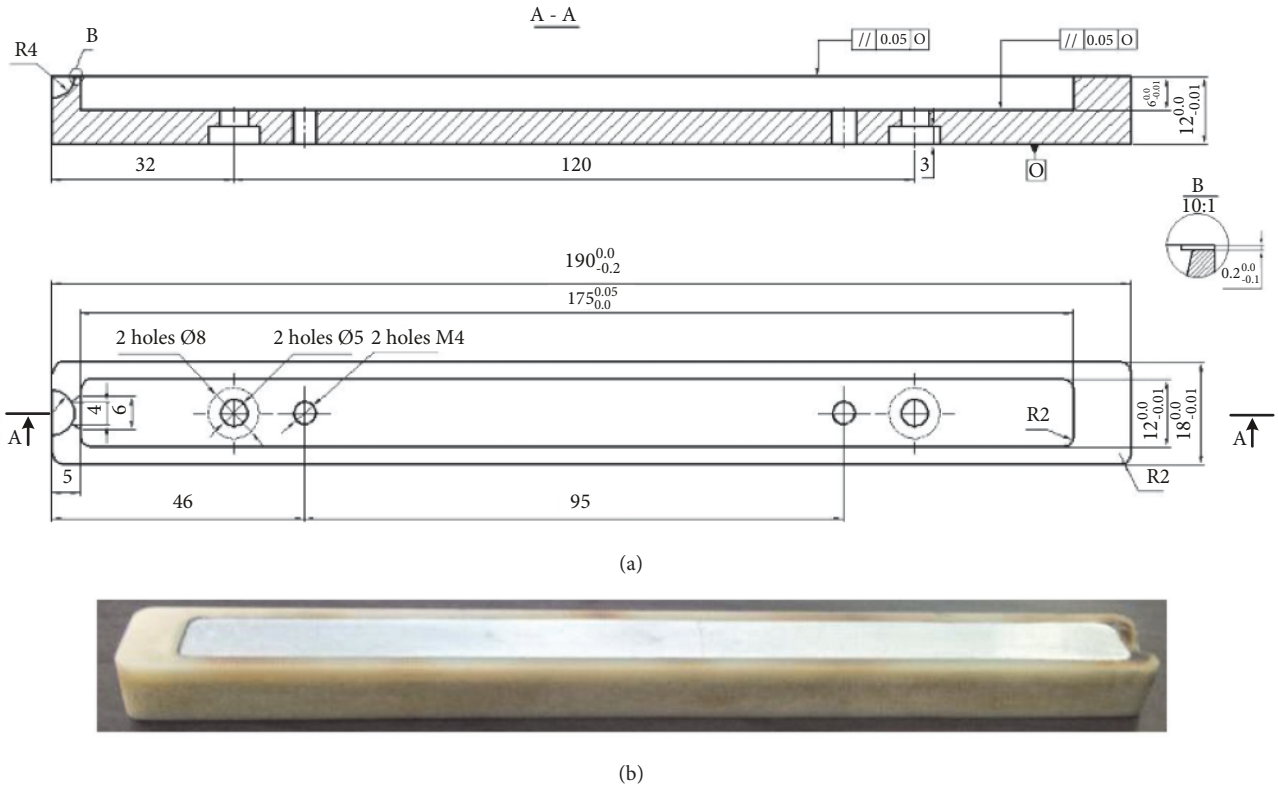


(a)

(b)

Figure 5: Mold insert for studying melt flow length. (a) Design of mold insert. (b) Experimental mold insert.

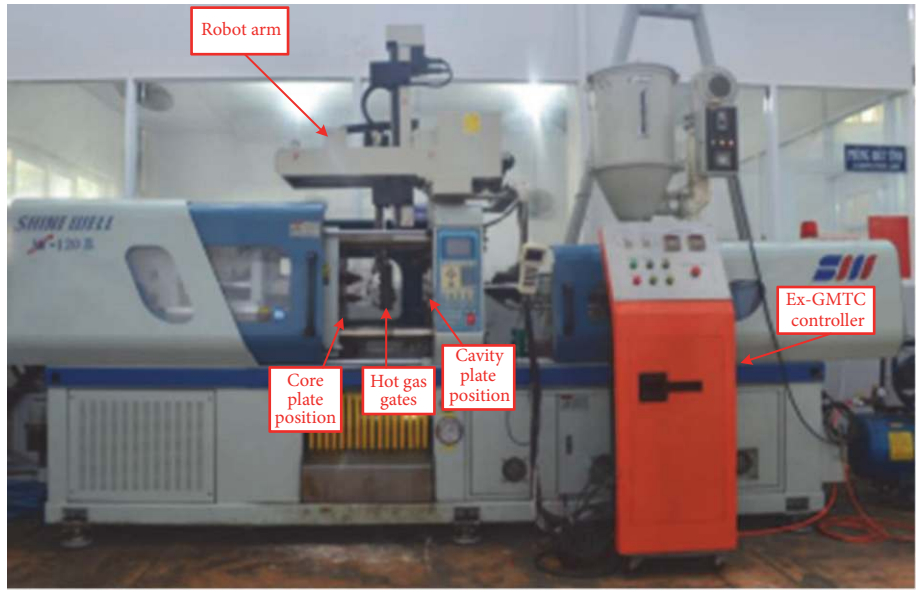


Figure 6: External gas-assisted mold temperature control experiment model.

this research, with Ex-GMTC used for the injection molding process, the heating process was observed in relation to the heating rate and temperature distribution within the cavity. To study the application of Ex-GMTC, the mold was designed as in Figure 4, with the gas drier having four hot gas gates. These gates were arranged along the cavity to improve the temperature distribution and heating rate. As an initial step, heating was simulated using the model, as in Figure 7. The heating process was performed at gas temperatures of 200°C, 250°C, 300°C, 350°C, and 400°C, a heating time of 30 s, and an initial cavity surface temperature of 30°C.

The simulation results show the temperature distribution of the cavity at the top view as in Figure 11 and the cross section A-A as in Figure 12. The temperature at the four

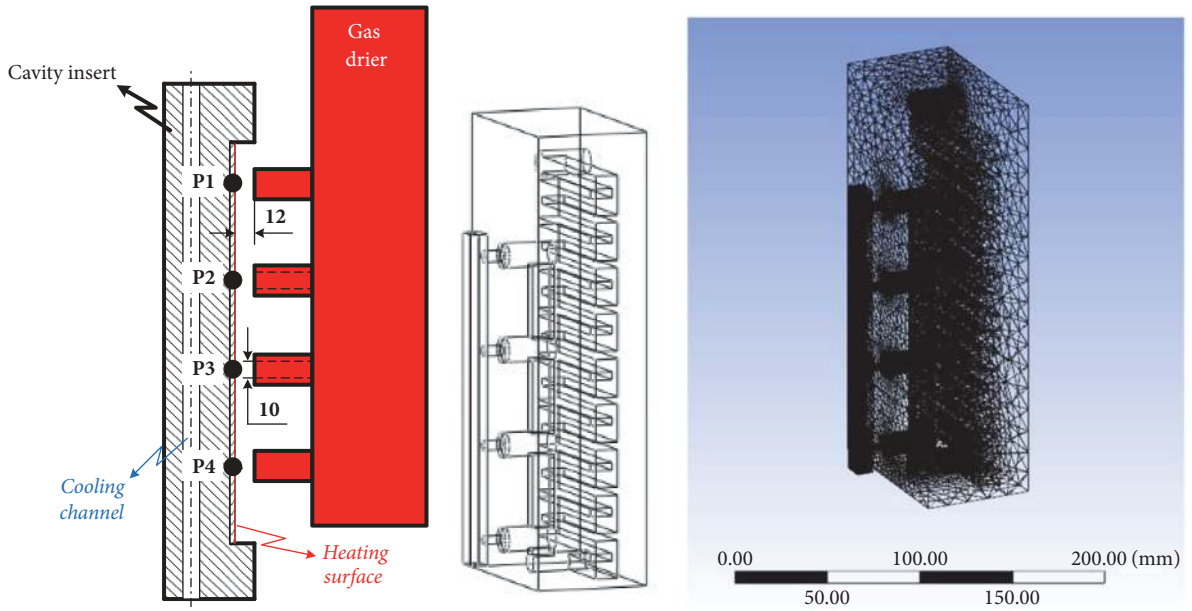


(a) Heating position (b) Simulation model (c) Meshing model

Figure 7: Model of Ex-GMTC with 4 gas gates.

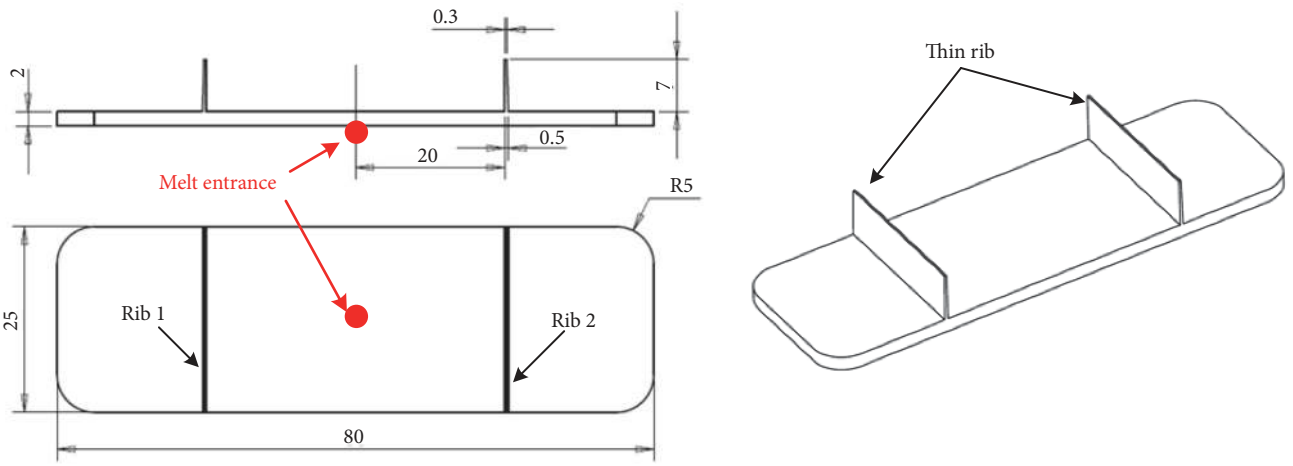


Figure 8: Thin rib model.

measurement points was collected as in Table 2. According to the temperature distribution simulation results, the cavity surface underwent a relatively balanced heating process, although there were some higher temperature regions near the hot gas gates. The differences in temperature are clearer at the beginning of the heating period because the heating rate at the gas gates was very strong during this period. This phenomenon is clear at all gas temperatures. By contrast, when a higher gas temperature was used (Figures 11(e) and 12), the difference in temperature is also clear at the end of heating period. This is because of an imbalance in the thermal energy between the receiving thermal energy (near the gas gates) and the calorific power area (distant from the gas gate). This phenomenon could be observed clearer with the temperature distribution at the cross section A-A as in Figure 12. At higher gas heating temperature, the cavity surface shows a trend of releasing greater calorific power to the environment. Therefore, in the area distant from the gas gate, the temperature was much lower than that of the area near the gas gate. This result could be observed clearly at a 400°C gas temperature and heating time of 30 s. To reduce this imbalance, the gas drier could be designed with more gas gates. However, as compared with other heating methods for injection molds [3, 8–10], the temperature distribution result shows that this heating method, with four gas gates and a cavity length of 175 mm, is highly advantageous. In addition, the effect of cavity insert was clarified by the appearing of higher temperature area at the cavity surface.

To assess heating rate, the temperatures at four points were collected and compared, as shown in Figure 13. According to the results, the raising of temperature showed a limitation of the heating process. The heating efficiency

Table 2: Simulation results of mold cavity temperature after heating for the melt flow length mold.

| Heating Time (s) | Position | Gas temperature (°C) | | | | |
|---|---|---|---|---|---|---|
| | | 200 | 250 | 300 | 350 | 400 |
| 5 | P1 | 62.3 | 73.2 | 83.3 | 92.5 | 102.8 |
| | P2 | 58.1 | 69.3 | 81.4 | 84.5 | 95.4 |
| | P3 | 56.6 | 67.2 | 79.8 | 82.4 | 91.3 |
| | P4 | 57.8 | 66.0 | 78.9 | 76.6 | 88.4 |
| 10 | P1 | 76.0 | 91.6 | 109.1 | 115.8 | 125.6 |
| | P2 | 78.3 | 92.6 | 109.5 | 115.5 | 126.8 |
| | P3 | 74.5 | 84.4 | 105.6 | 104.3 | 115.7 |
| | P4 | 74.4 | 86.8 | 104.4 | 105.1 | 115.6 |
| 15 | P1 | 90.8 | 105.7 | 119.0 | 131.8 | 148.4 |
| | P2 | 87.2 | 102.7 | 117.5 | 123.7 | 144.2 |
| | P3 | 86.6 | 101.5 | 116.3 | 124.2 | 142.1 |
| | P4 | 85.5 | 101.3 | 115.4 | 131.0 | 141.6 |
| 20 | P1 | 92.2 | 114.0 | 125.6 | 147.8 | 154.8 |
| | P2 | 90.2 | 110.9 | 122.9 | 146.6 | 153.7 |
| | P3 | 88.3 | 108.1 | 119.7 | 145.9 | 151.1 |
| | P4 | 84.8 | 105.3 | 117.1 | 145.9 | 150.5 |
| 25 | P1 | 95.6 | 116.2 | 129.8 | 147.4 | 160.1 |
| | P2 | 92.1 | 112.4 | 125.5 | 144.0 | 158.6 |
| | P3 | 91.2 | 112.6 | 123.3 | 142.1 | 157.8 |
| | P4 | 86.6 | 96.8 | 117.4 | 143.8 | 155.7 |
| 30 | P1 | 96.5 | 119.6 | 132.9 | 151.7 | 161.3 |
| | P2 | 94.4 | 117.7 | 128.0 | 147.9 | 159.4 |
| | P3 | 94.3 | 116.9 | 127.4 | 145.3 | 158.1 |
| | P4 | 84.0 | 106.2 | 119.6 | 140.7 | 152.5 |

was high only at the beginning of the heating step; after 20 s, the temperature increase was slowed. This result was because of heat convection between the hot gas and the mold surface. At the same gas temperature, when the cavity temperature increased, the transfer of thermal energy was lower. Therefore, with the four gas temperatures, highly efficient heating was achieved within the first 20 s, with a maximum heating rate of 6.4°C/s with the 400°C gas. In this case, although there is a limitation in the raising of temperature, the mold surface reached 158.4°C, which was sufficiently high for almost all of the melt to flow easily into the cavity. By contrast, this limitation reduced overheating of the mold insert, especially with micro injection molding. This is also an advantage of Ex-GMTC as compared with other heating methods for injection molds [10–14].

To verify the accuracy of the simulation result, the experiment was conducted with the same boundary conditions as used in the simulation. The experiment was conducted 10 times for each case and the average value is presented herein. The temperatures at four points (Figure 7(a)) were collected using a thermal camera and compared with the simulation results, as shown in Figure 13. Based on these comparisons, the temperature difference between the simulations and experiments was lower than 12°C. This difference is because of a measurement delay of the thermal camera, especially as the thermal energy can transfer quickly from the high temperature area to the lower temperature area. However, in general, this result demonstrates that the simulations and experiments showed good agreement. In addition, the limitation in the heating process was observed experimentally.

*3.2. Effect of External Gas-Assisted Mold Temperature Control on Melt Flow Length.* In injection molding, cavity surface temperature has a strong influence on melt flow length because of a reduction of the freeze layer [1, 5]. This property is a key aspect of the molding process, especially with micro products or thin-walled components. In this study, to increase the cavity temperature, Ex-GMTC was applied to the melt flow length mold, as in Figure 4. To observe the effect of Ex-GMTC on the melt flow length, the heating step was achieved at a gas temperature of 400°C and the heating time was varied from 5 to 20 s. After the heating step, the gas drier was moved outside the molding area and the two-half mold plate was closed for the filling step to commence (Step 3 in Figure 1). In this period, the mold temperature will change, and the mold temperature at the end of this period impacts the melt flow length. In the real molding cycle, it takes about 6 s from the end of the heating period to the start of the filling step. Therefore, after the heating period was finished, the mold temperature was measured for comparison with the melt filling result. For the molding experiment, polypropylene (PP 1100N from Advanced Petrochemical Company) and acrylonitrile butadiene styrene (ABS 750SW from Kumho Petrochemical

Table 3: Molding parameters for the melt flow length experiment.

| No. | Molding parameters | Value | |
|---|---|---|---|
| | | PP material | ABS material |
| 1 | Melt temperature | 210°C | 230°C |
| 2 | Injection pressure | 60 kg/cm$^2$ | |
| 3 | Cooling time | 20 s | |
| 4 | Injection speed | 50 mm/s | |
| 5 | Injection time | 0.5 s | |
| 6 | Packing time | 2.5 s | |
| 7 | Heating time | 5 s, 10 s, 15 s, 20 s | |
| 8 | Initial mold temperature | 30°C | |
| 9 | Glass transition temperature | 100°C | 105°C |

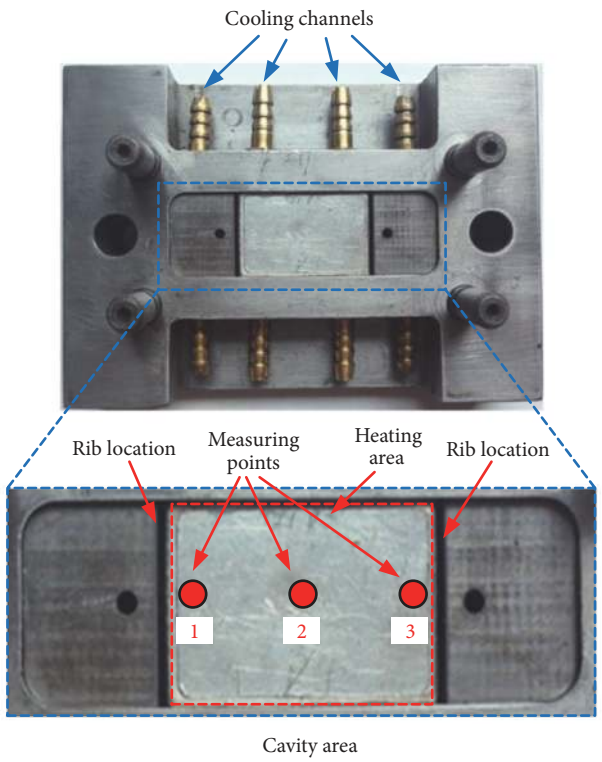


Figure 9: Mold plate of thin rib with the cavity insert.

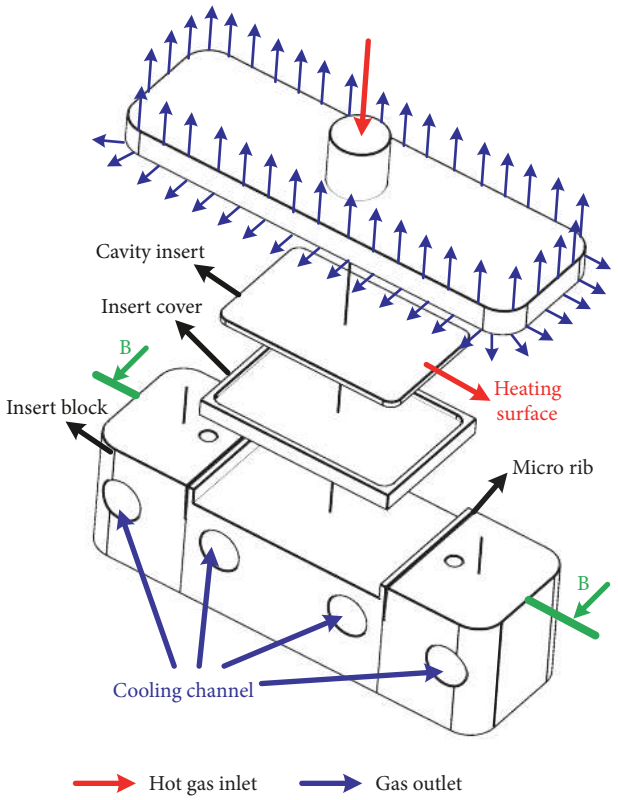


Figure 10: Simulation model of thin rib heating step.

Company) were used with the material properties as in Table 3.

Using the infrared camera, we determined the temperature distribution of the melt flow length mold (Figure 14). This shows that with heating times of 5, 10, 15, and 20 s, at the beginning of melt filling step, the temperature of the cavity surface is maintained at 62.8°C, 94.9°C, 121.2°C, and 133.7°C, respectively. In addition, the uniformity of the temperature distribution was clearly improved after the heating step. This result could be explained by the heat conduction of the mold insert. In this period, the thermal energy would have transferred from the higher temperature region to the lower temperature region. Therefore, the temperature distribution of the mold insert would be more uniform. In the experiment, the temperature difference was less than 5°C for all cavity areas (175 mm × 12 mm). This degree of temperature uniformity is much improved over that of our former research [15–17] and could help reduce the warpage of plastic products. The result also indicates that with a proper layout of the gas gates, Ex-GMTC could be applied to the complex geometry of the mold cavity.

Experimentally, the molding process was operated with different heating times. The plastic components were evaluated, as shown in Figures 15 and 16. With the plastic material and molding parameters shown in Table 3, the experiment was performed with melt flow thicknesses of 0.2, 0.4, and 0.6 mm. The results show that the melt flow length was improved

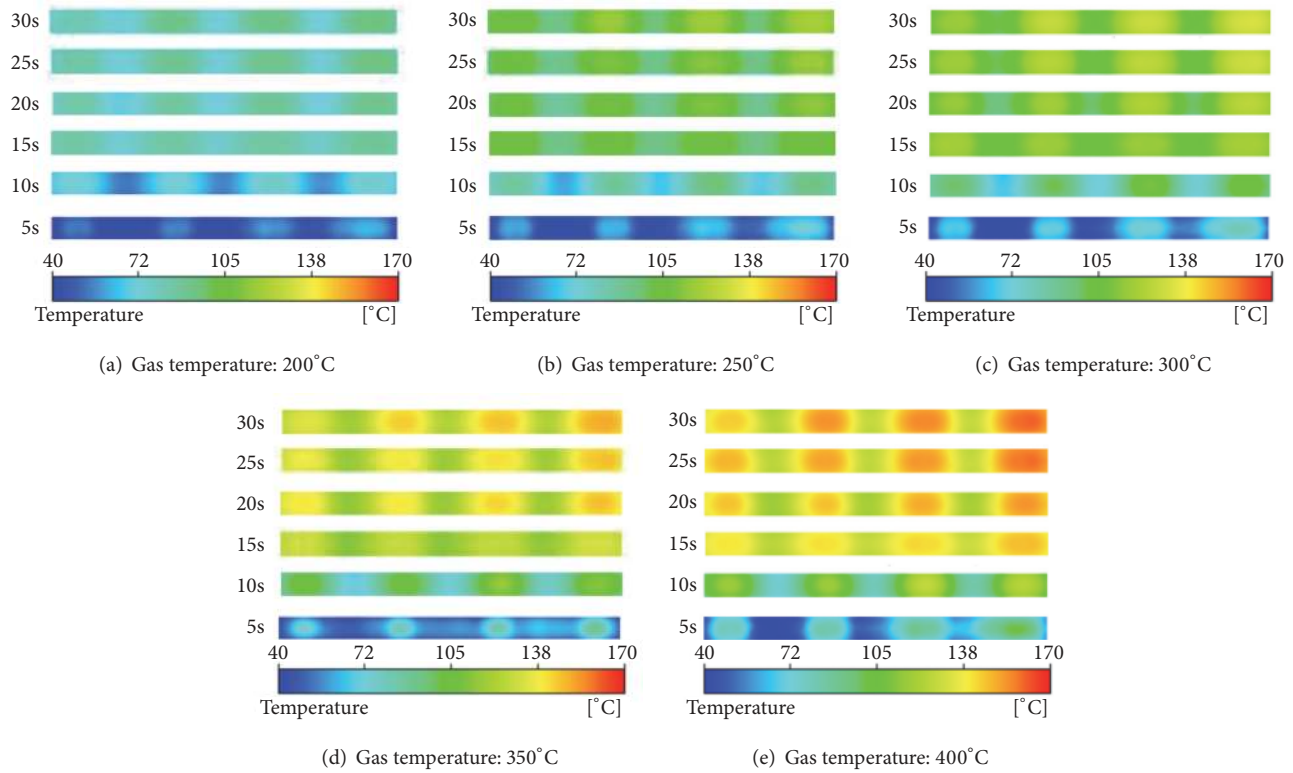


Figure 11: Temperature distribution at the cavity surface of the melt flow length mold after 30 s heating at different gas temperatures.

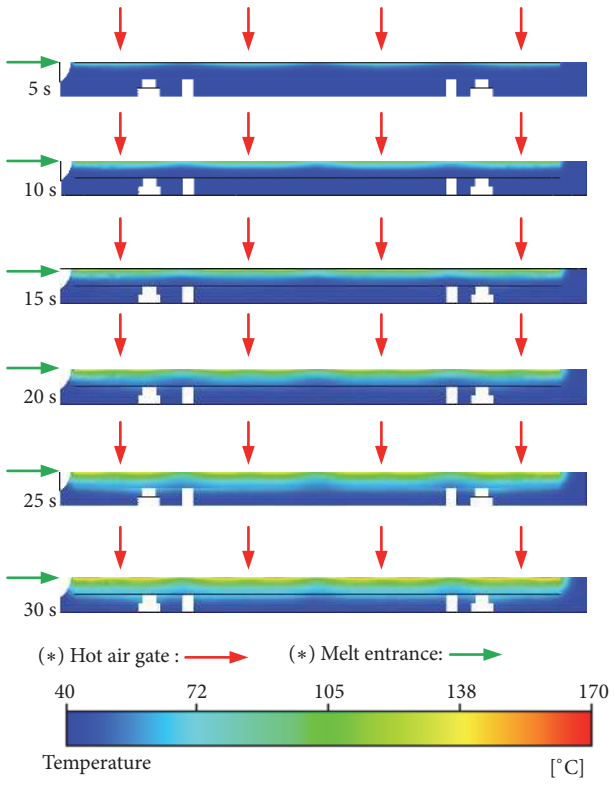


Figure 12: Temperature distribution at the cross section A-A with the gas heating of 400°C.

with the application of Ex-GMTC and a heating time between 5 and 20 s. The improvement is clearer with heating times of 15 and 20 s because the cavity surface temperature was heated to over 110°C in these cases, which is higher than the glass transition temperature of both the PP and ABS materials (Table 4). The percentage improvement in flow length was calculated and is shown in Figure 17. The results show that by applying Ex-GMTC for a 0.6 mm flow thickness, the melt flow length could be improved by 23.5% with the PP material and 22.3% with the ABS material. With the 0.2 mm flow thickness, the flow length increased from 37.85 to 41.32 mm with the PP material and from 14.54 to 15.8 mm with the ABS material.

*3.3. Improving the Thin Rib Filling Step by External Gas-Assisted Mold Temperature Control.* To assess the efficiency of Ex-GMTC on the injection molding cycle, the mold for a thin rib product was used. The dimensions of this product are shown in Figure 8, with rib thickness varied from 0.3 to 0.5 mm and a rib height of 7.0 mm. The melt material was ABS. For the common injection molding process, mold temperature should be set in the range 20°C to 80°C. However, with a thin wall product, the mold temperature must be set as high as possible to allow for complete filling of the cavity. This readily allows flow because of the reduction of the freeze layer of the melt flow [5]. However, when the mold temperature is high, energy wastage will also be high; in addition, other issues such as warpage and flashing can become evident. To mitigate such

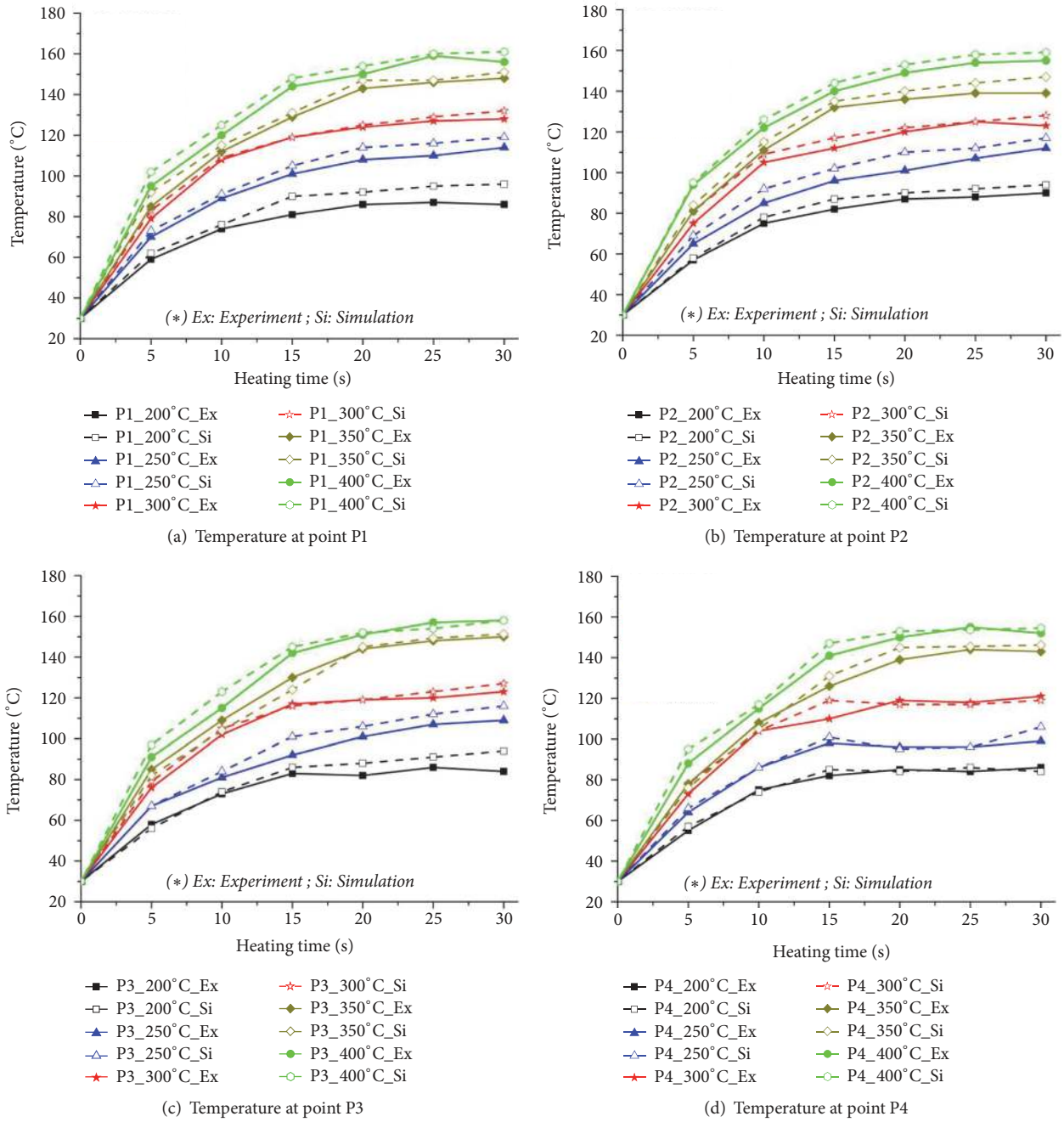


(a) Temperature at point P1

(b) Temperature at point P2

(c) Temperature at point P3

(d) Temperature at point P4

FIGURE 13: Temperature history at four points with different gas sources.

issues, local mold temperature control was presented in this study with the Ex-GMTC method. Rather than maintaining all mold plates at a high temperature, Ex-GMTC is applied to the cavity area by local gas preheating at the beginning of the molding cycle. The high temperature at the cavity center will reduce the pressure drop of the melt flow as it enters the mold cavity [2, 4]. Figure 9 shows the cavity plate, which includes the cavity area and the melt entrance area.

With the above structure, the area at the cavity center was redesigned with a steel insert to improve the heating efficiency. This insert had dimensions of $40 \times 25 \times 1.0\ mm^3$. A gas drier with one gate and a gas temperature of 400°C were used for these experiments. To observe the influence of Ex-GMTC on the filling step of the thin rib, the common molding cycle was initially operated with molding temperatures from 45°C to 75°C. In these cases, the mold temperature controller was used with water flow inside the cooling channel. Then, Ex-GMTC was applied with heating times from 4 to 10 s. After the heating step, the melt was filled into the cavity after 6 s for the mold closing. All thin rib experiments used the same ABS material shown in Table 3.

To study the heating step for the thin rib mold, the temperature of the cavity surface was measured at three points, as shown in Figure 9. By experiment, the temperature

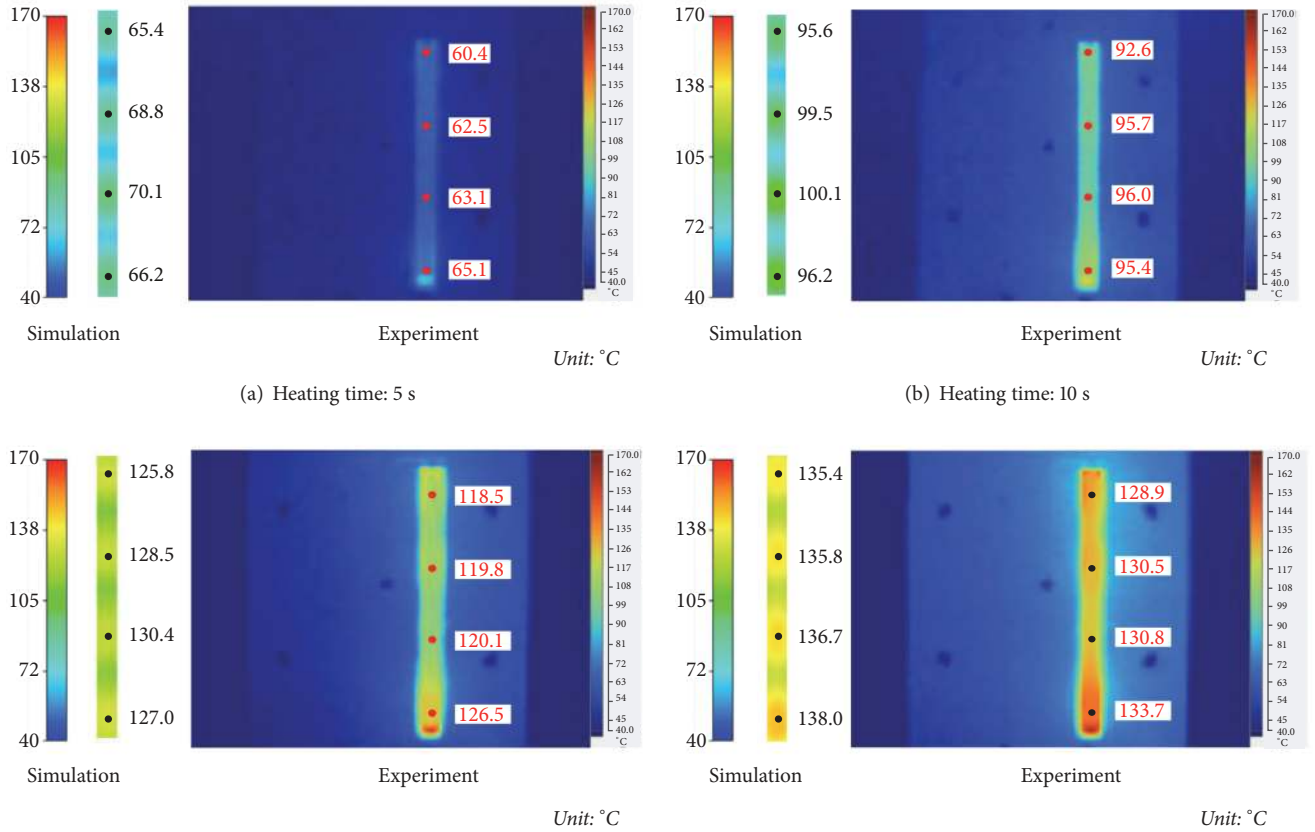


FIGURE 14: Temperature distribution of the melt flow mold at the beginning of melt filling step.

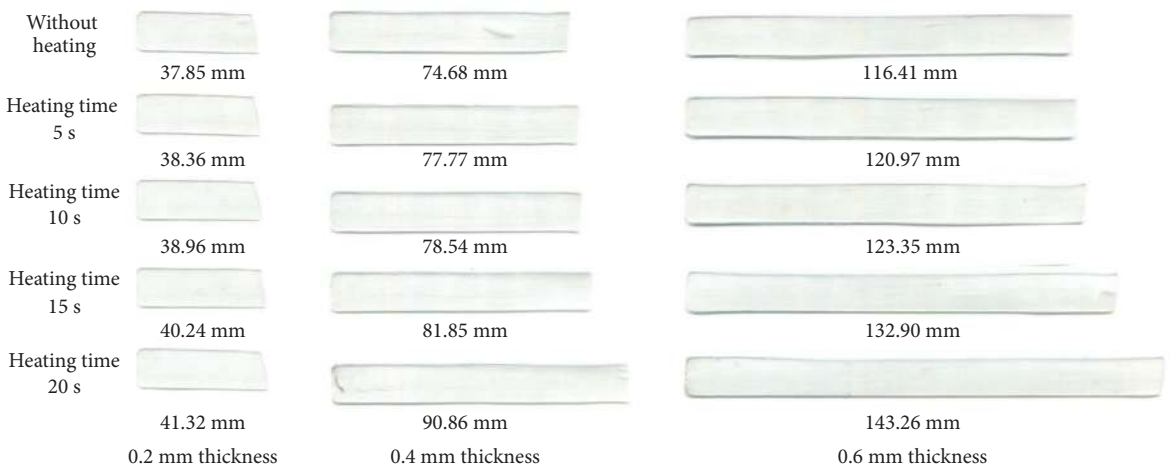


FIGURE 15: Experimental results for melt flow length with the polypropylene material at different heating times.

histories are given in Table 4 and Figure 18. The temperature histories in Figure 18 show that at the end of the heating step the mold temperature reached 112.0, 121.3, 132.5, and 140.8°C at heating times of 4, 6, 8, and 10 s, respectively. In addition, after 6 s for mold closure, the temperature of the heating surface decreased by about 10°C with the thin rib mold. To verify the temperature uniformity, the thermal camera was used to determine the temperature distribution in the thin rib mold at the end of the heating step. These results are shown in Figure 20. The results show that the temperature uniformity was very good, and the heating process influences only the heating area. For observing the temperature distribution and uniformity along the thickness of mold, the heating step was simulated with the gas heating of 400°C and the simulation


Figure 16: Experimental results for melt flow length with the acrylonitrile butadiene styrene material at different heating times.

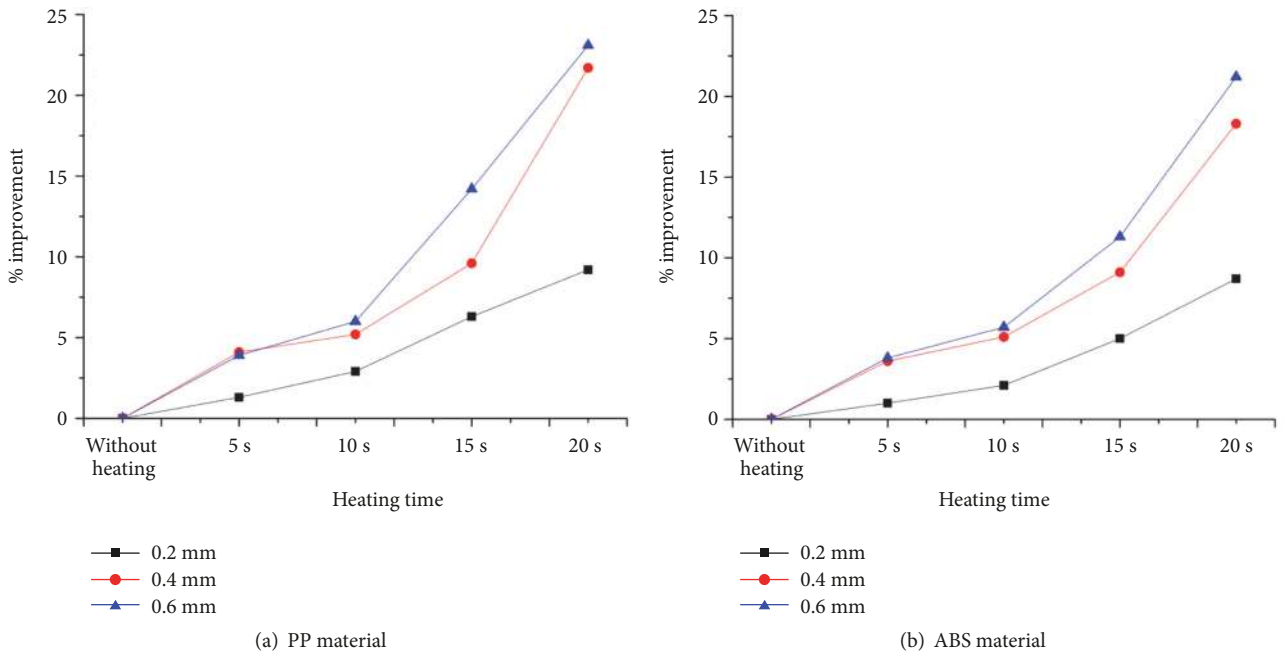


Figure 17: Improvement of melt flow length with the polypropylene and acrylonitrile butadiene styrene materials at different heating time.

model as in Figure 10. The temperature distribution at the cross section B-B was shown in Figure 19. According to this result, the highest temperature was located at the center surface of cavity insert. The mold surface of the rib is not close to the gas heating gate, so, the heating effect is not as clear as the cavity insert. Both simulation and experimental results show that the temperature difference between the three points was less than 10°C. The temperature difference between Point 1 and Point 3 was lower than 3.2°C. The more consistent the temperature between Points 1 and 3, the more balanced the melt filling into the two ribs. In addition, the temperature at the center heating area (Point 2) was always higher than that at the other points. This is because of the closer proximity of the gas gate to Point 2 than to the other points.

At each mold temperature, the molding cycle was performed 20 times to reach system stability, before the next

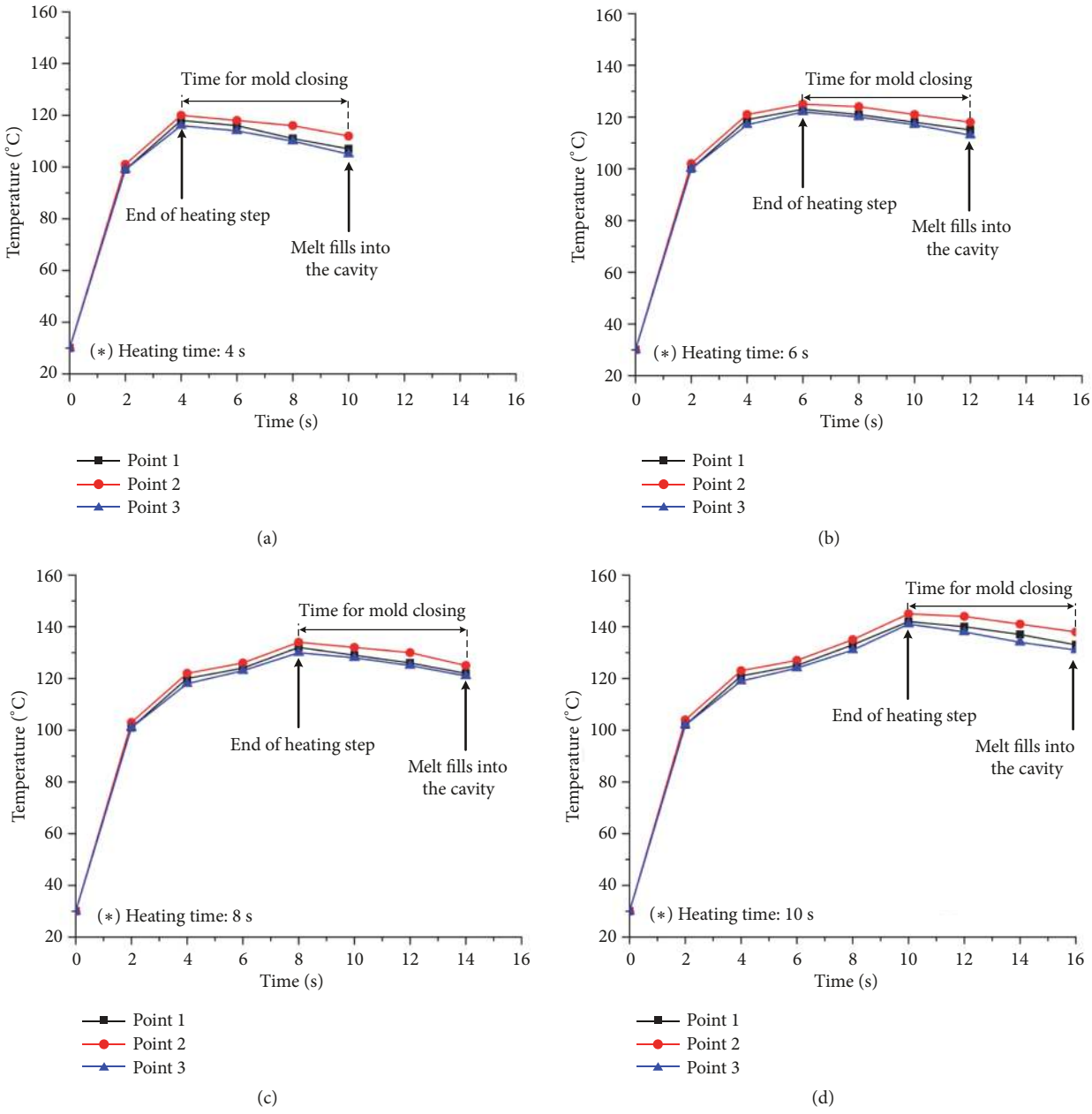


Figure 18: Temperature histories of the thin rib mold surface at three points.

10 cycles were used for comparing rib height. After the molding step, the molding samples were collected and rib heights measured. The results are shown in Figures 21 and 22. According to these results, when the mold temperature increased from 45°C to 75°C, the rib height increased from 2.8 to 4.2 mm. When Ex-GMTC was used with 400°C gas, although the highest temperature was focussed on the cavity insert (Figure 19), the improvement of thin rib was observed clearly. In detail, when the mold temperature varied from 112.0°C to 140.8°C, the thin rib height reached a maximum of 7.0 mm. This development is due to the reduction of the frozen layer when the melt flows through the cavity insert, which helps to increase the filling pressure at the thin rib area. Figure 22 also shows that the height of two ribs was different when using the mold temperature controller with hot water flow inside the cooling channel. This is because of the nonsymmetry of the mold structure; the temperature distribution inside the mold was impacted, especially in the lower mold temperature case. On the contrary, with Ex-GMTC, the heating only affected the molding surface; therefore, the mold structure had almost no influence on the heating result. As such, the height of two thin ribs was more uniform than with the hot water control method.

## 4. Conclusions

In this research, external gas-assisted mold temperature control (Ex-GMTC) was applied to the injection molding

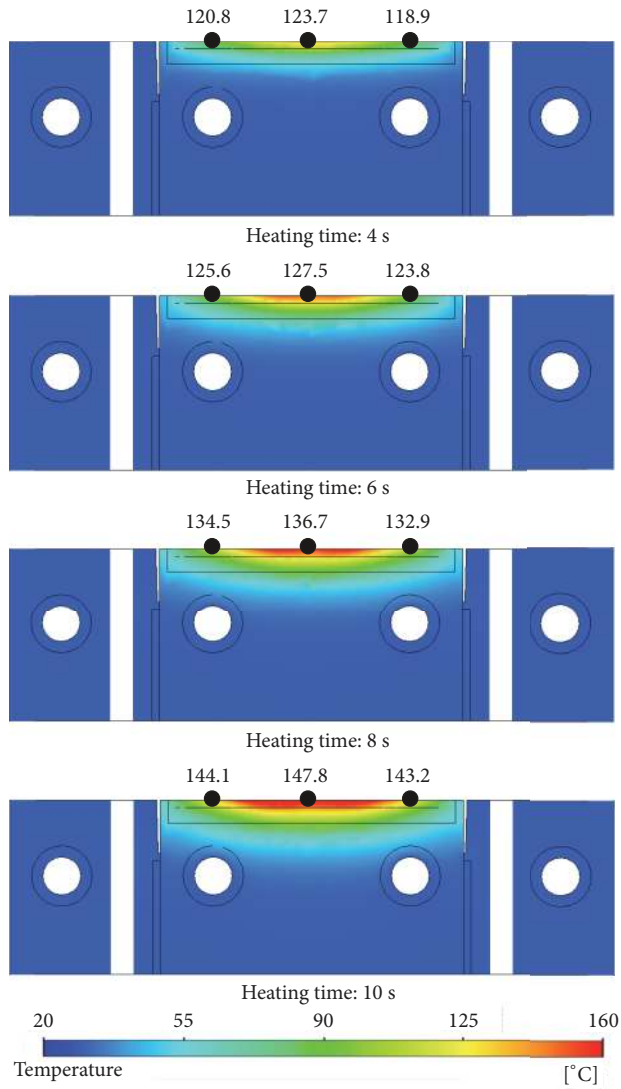


Figure 19: Temperature distribution at the cross section B-B with the thin rib model.

cycle to improve mold filling ability. The simulations and experiments were performed with molds of melt flow length and thin rib. For the mold of melt flow length, the gas temperature was varied from 200°C to 400°C and the molding cycle was operated at component thicknesses of 0.2, 0.4, and 0.6 mm. With the thin rib mold, Ex-GMTC was performed using 400°C gas at the center of the cavity. The filling of melt into the thin rib was observed when using (i) a mold temperature controller with hot water flowing inside the cooling channel and (ii) Ex-GMTC. Based on the results, the following conclusions were obtained:

(i) With a length of 175 mm, the cavity surface of the melt flow length mold showed a relatively balanced heating process when using four hot gas gates, although there were some higher temperature regions near the gates. Heating efficiency was high at the beginning of the heating step; however, after 20 s, the temperature increase slowed. This result was because of heat convection between the hot gas and the mold surface. The highest heating rate achieved was 6.4°C/s with the 400°C gas.

(ii) Because of heat convection, the simulations and experiments showed that Ex-GMTC has a limitation in terms of heating efficiency. Nevertheless, with the melt flow length mold, the mold surface reached 158.4°C, at which temperature almost all of the melt could flow easily into the cavity.

(iii) By applying Ex-GMTC for the 0.6 mm flow thickness, the melt flow length could be improved by 23.5% with the PP material and 22.3% with the ABS material. With the 0.2-mm flow thickness, the flow length also increased from 37.85 to 41.32 mm with the PP material and from 14.54 to 15.8 mm with the ABS material.

(iv) With the thin rib mold, when the mold temperature increased from 45°C to 75°C, the rib height was increased from 2.8 to 4.2 mm. When the Ex-GMTC

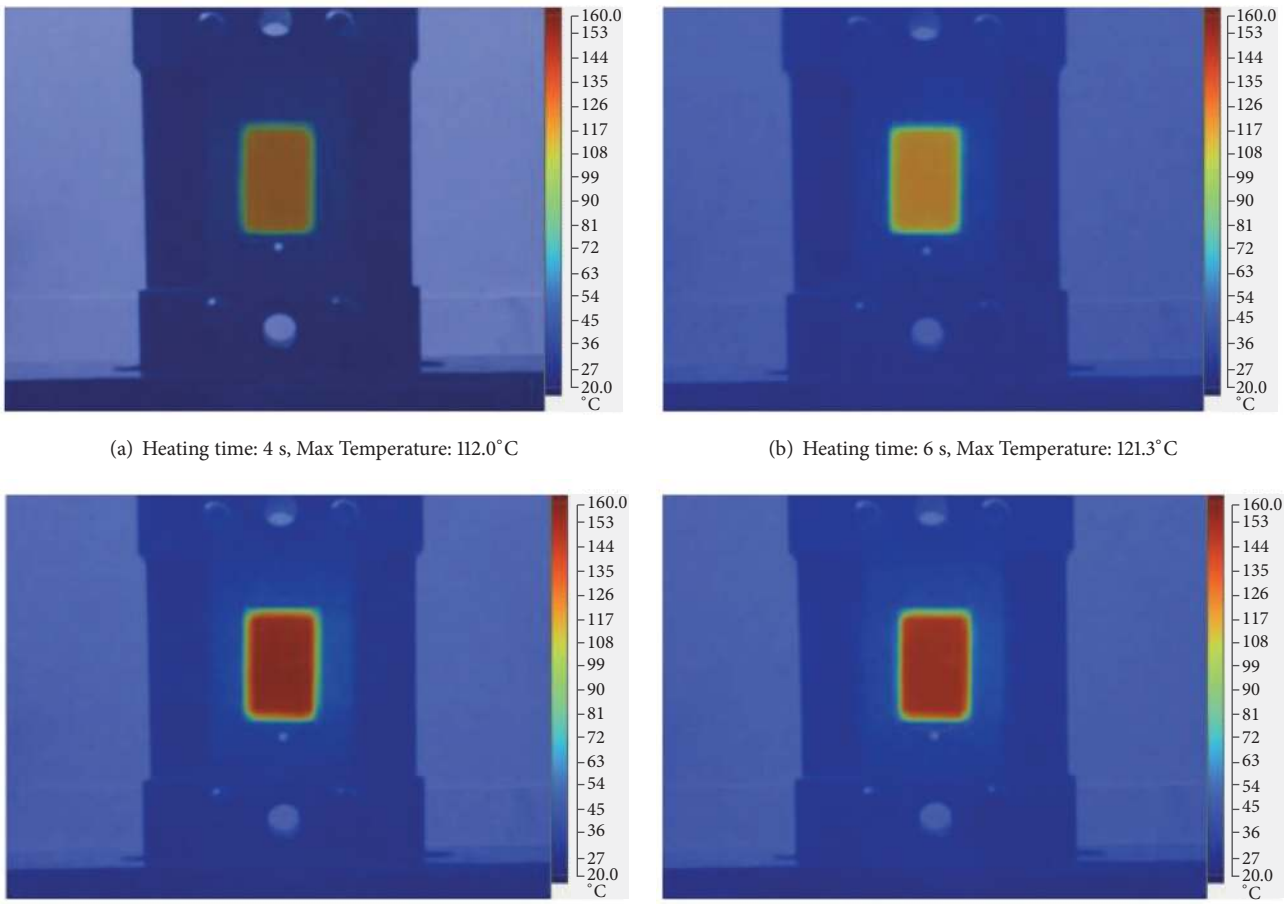


(a) Heating time: 4 s, Max Temperature: 112.0°C

(b) Heating time: 6 s, Max Temperature: 121.3°C

(c) Heating time: 8 s, Max Temperature: 132.5°C

(d) Heating time: 10 s, Max Temperature: 140.8°C

Figure 20: Temperature distribution at the end of the heating step for the thin rib cavity at different heating times.

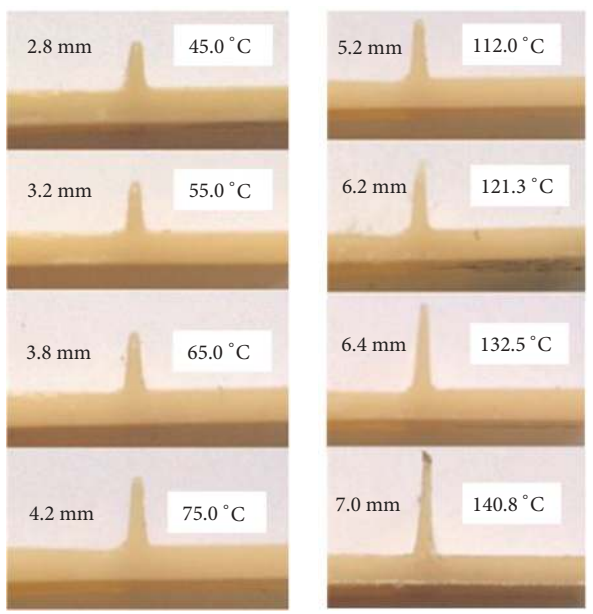


(a) Mold temperature control with the hot water

(b) Mold temperature control with Ex-GMTC

Figure 21: Measurement of thin rib height at different cavity temperatures.

Table 4: Experimental results for cavity temperature with the thin rib mold at different heating times.

| Measuring point | Measuring time (s) | Heating time (s) | | | |
|---|---|---|---|---|---|
| | | 4 | 6 | 8 | 10 |
| 1 | 0 | 30 | 30 | 30 | 30 |
| | 2 | 99.2 | 100.2 | 101.2 | 102.2 |
| | 4 | 118.6 | 119.9 | 120.1 | 121.1 |
| | 6 | 116.4 | 123.4 | 124.2 | 125.6 |
| | 8 | 111.1 | 121.5 | 132.6 | 133.5 |
| | 10 | 107.0 | 118.0 | 129.5 | 142.3 |
| | 12 | | 115.5 | 126.7 | 140.8 |
| | 14 | | | 122.0 | 137.2 |
| | 16 | | | | 133.0 |
| 2 | 0 | 30 | 30 | 30 | 30 |
| | 2 | 101.2 | 102.1 | 103.3 | 104.2 |
| | 4 | 120.6 | 121.9 | 122.2 | 123.6 |
| | 6 | 118.5 | 125.5 | 126.6 | 127.2 |
| | 8 | 116.7 | 124.4 | 134.7 | 135.1 |
| | 10 | 112.1 | 121.9 | 132.4 | 145.8 |
| | 12 | | 118.4 | 130.2 | 144.2 |
| | 14 | | | 125.1 | 141.6 |
| | 16 | | | | 138.1 |
| 3 | 0 | 30 | 30 | 30 | 30 |
| | 2 | 99.2 | 100.3 | 101.2 | 102.3 |
| | 4 | 116.2 | 117.5 | 118.3 | 119.9 |
| | 6 | 114.1 | 122.4 | 123.4 | 124.8 |
| | 8 | 110.4 | 120.1 | 130.5 | 131.1 |
| | 10 | 105.6 | 117.2 | 128.9 | 141.4 |
| | 12 | | 113.2 | 125.7 | 138.3 |
| | 14 | | | 121.1 | 134.5 |
| | 16 | | | | 131.1 |
| Heating time | | | | Mold closing time | |

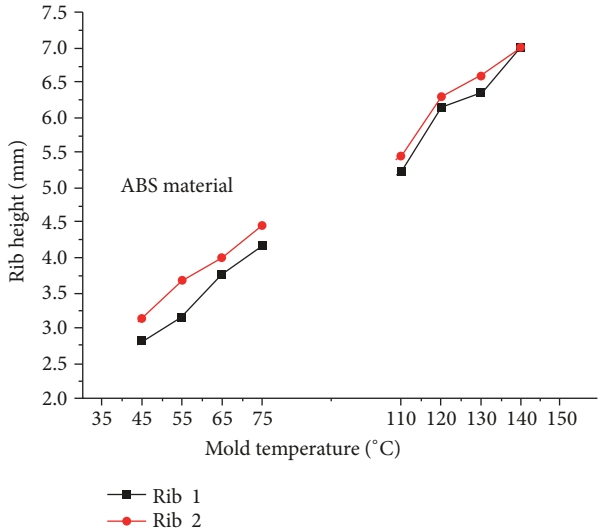


Figure 22: Improvement of thin rib height at different cavity temperatures.

was used, the mold temperature varied from 112.0°C to 140.8°C and the thin rib height reached 7.0 mm. Because the Ex-GMTC was not influenced by mold structure, the heating method supported a better temperature distribution than that of the hot water controller method; as a result, a better balance in melt flow could be achieved.

## Data Availability

The data used to support the findings of this study are available from the corresponding author upon request.

## Conflicts of Interest

The authors declare that they have no conflicts of interest.

## Authors' Contributions

Phan The Nhan and Pham Son Minh conceived of the presented idea and developed the simulation and experimental methods. Phan The Nhan and Thanh Trung Do verified the simulation results. All authors discussed the results and contributed to the final manuscript.

## Acknowledgments

This research was supported by the Ministry of Education and Training, Vietnam; the Ministry of Science and Technology, Vietnam; and HCMC University of Technology and Education, Hochiminh City, Vietnam. The authors are grateful to Mr. Nguyen Ho, Mr. Bui Huu Manh, Mr. Nguyen Thanh Nhan, Mr. Dang Ngoc Son, and Mr. Tran Van Tron for their help in conducting the study experiments.

## References

[1] L. Zema, G. Loreti, A. Melocchi, A. Maroni, and A. Gazzaniga, "Injection molding and its application to drug delivery," *Journal of Controlled Release*, vol. 159, no. 3, pp. 324–331, 2012.

[2] M. Vázquez and B. Paull, "Review on recent and advanced applications of monoliths and related porous polymer gels in micro-fluidic devices," *Analytica Chimica Acta*, vol. 668, no. 2, pp. 100–113, 2010.

[3] M.-S. Huang and Y.-L. Huang, "Effect of multi-layered induction coils on efficiency and uniformity of surface heating," *International Journal of Heat and Mass Transfer*, vol. 53, no. 11-12, pp. 2414–2423, 2010.

[4] S.-C. Nian, C.-Y. Wu, and M.-S. Huang, "Warpage control of thin-walled injection molding using local mold temperatures," *International Communications in Heat and Mass Transfer*, vol. 61, no. 1, pp. 102–110, 2015.

[5] S. Meister and D. Drummer, "Affecting the ageing behaviour of injection-moulded microparts using variothermal mould tempering," *Advances in Mechanical Engineering*, vol. 2013, Article ID 407964, 7 pages, 2013.

[6] F. Baruffi, M. Calaon, and G. Tosello, "Effects of micro-injection moulding process parameters on accuracy and precision of thermoplastic elastomer micro rings," *Precision Engineering*, vol. 51, pp. 353–361, 2018.

[7] M.-C. Jeng, S.-C. Chen, P. S. Minh, J.-A. Chang, and C.-S. Chung, "Rapid mold temperature control in injection molding by using steam heating," *International Communications in Heat and Mass Transfer*, vol. 37, no. 9, pp. 1295–1304, 2010.

[8] W. Guilong, Z. Guoqun, L. Huiping, and G. Yanjin, "Analysis of thermal cycling efficiency and optimal design of heating/cooling systems for rapid heat cycle injection molding process," *Materials & Design*, vol. 31, no. 7, pp. 3426–3441, 2010.

[9] S. Liparoti, A. Sorrentino, and G. Titomanlio, "Fast cavity surface temperature evolution in injection molding: control of cooling stage and final morphology analysis," *RSC Advances*, vol. 6, pp. 99274–99281, 2016.

[10] P.-C. Chang and S.-J. Hwang, "Simulation of infrared rapid surface heating for injection molding," *International Journal of Heat and Mass Transfer*, vol. 49, no. 21-22, pp. 3846–3854, 2006.

[11] S.-C. Chen, W.-R. Jong, Y.-J. Chang, J.-A. Chang, and J.-C. Cin, "Rapid mold temperature variation for assisting the micro injection of high aspect ratio micro-feature parts using induction heating technology," *Journal of Micromechanics and Microengineering*, vol. 16, no. 9, pp. 1783–1791, 2006.

[12] D. Yao, T. E. Kimerling, and B. Kim, "High-frequency proximity heating for injection molding applications," *Polymer Engineering & Science*, vol. 46, no. 7, pp. 938–945, 2006.

[13] S.-C. Chen, P. S. Minh, J.-A. Chang, S.-W. Huang, and C.-H. Huang, "Mold temperature control using high-frequency proximity effect induced heating," *International Communications in Heat and Mass Transfer*, vol. 39, no. 2, pp. 216–223, 2012.

[14] H.-L. Lin, S.-C. Chen, M.-C. Jeng, P. S. Minh, J.-A. Chang, and J.-R. Hwang, "Induction heating with the ring effect for injection molding plates," *International Communications in Heat and Mass Transfer*, vol. 39, no. 4, pp. 514–522, 2012.

[15] S.-C. Chen, R.-D. Chien, S.-H. Lin, M.-C. Lin, and J.-A. Chang, "Feasibility evaluation of gas-assisted heating for mold surface temperature control during injection molding process," *International Communications in Heat and Mass Transfer*, vol. 36, no. 8, pp. 806–812, 2009.

[16] S.-C. Chen, C.-Y. Lin, J.-A. Chang, and P. S. Minh, "Gas-assisted heating technology for high aspect ratio microstructure injection molding," *Advances in Mechanical Engineering*, vol. 2013, Article ID 282906, 10 pages, 2013.

[17] S.-C. Chen, P. S. Minh, and J.-A. Chang, "Gas-assisted mold temperature control for improving the quality of injection molded parts with fiber additives," *International Communications in Heat and Mass Transfer*, vol. 38, no. 3, pp. 304–312, 2011.

[18] H. D. Baehr and K. Stephan, *Heat and Mass Transfer*, Springer, New York, 2nd edition, 2006.